

# Impact of the Coulomb Interaction on Nano-Scale Silicon Device Characteristics

Nobuyuki Sano

Received: October 4, 2010/ Accepted: date

**Abstract** Monte Carlo simulations coupled self-consistently with the three-dimensional Poisson equation are carried out under the double-gate MOSFET structures. The Coulomb force experienced by an electron inside the device is directly evaluated by performing the Monte Carlo simulations with or without the full Coulomb interaction and the Coulomb force on the channel electron corresponding to plasmon excitations is clarified. It is pointed out that the consistency of the boundary condition is achieved only if the long-range Coulomb interaction is properly taken into account, and this is crucial for predicting reliable device characteristics in ultra-small devices. The drain current and transconductance are greatly degraded if the self-consistent potential fluctuations are taken into account.

**Keywords** quasi-ballistic transport · Monte Carlo · device simulation · Coulomb interaction · MOSFET

## 1 Introduction

It has been pointed out that the Coulomb interaction among the electrons in the channel region and/or those in the high-doped regions in nano-scale MOSFETs is expected to be of crucial importance to predict reliable device characteristics [1]. This is because the channel is sandwiched with heavily doped source and drain regions in the distance of tens nm and the Coulomb interaction directly affects the transport properties in the channel region [2]. As a result, transport simulations coupled self-consistently with the Poisson equation be-

comes mandatory for any reliable simulations of device performance of ultra-small MOSFETs [3].

Incorporation of the Coulomb interaction in any particle-based simulations, however, has been a long-standing issue. It has been tackled with various techniques such as Molecular Dynamics (MD) simulations [4, 5], Particle-Particle-Particle-Mesh (P<sup>3</sup>M) method [6, 7], and the Monte Carlo (MC) method [8]. As far as the MC approach is concerned, the most advanced treatment of the Coulomb interaction so far would be due to Fischetti and Laux [9, 1], by which both the long-range and short-range parts of the Coulomb interaction have been introduced into MC simulations with very careful consideration of the dimensionality and the mesh size. Unfortunately, their MC simulations have been two-dimensional. Yet, the potential fluctuations associated with the Coulomb interaction are intrinsically three-dimensional (3D) and, thus, 3D MC simulation is desired for quantitative analyses. We have recently extended their approach to 3D MC simulations including the Coulomb interaction as accurately as possible [10, 11]. In the present paper, we introduce double-gate (DG) MOSFET structures into our MC simulator and investigate quantitatively the effects of the Coulomb interaction on device characteristics of nanoscale DG-MOSFETs.

## 2 Simulation Method and Device Structure

The MC method coupled self-consistently with the Poisson equation is employed. All relevant scattering processes such as acoustic and optical phonon scattering, impurity scattering, and the short-range electron-electron scattering are included under the framework of the non-parabolic band structure of Si. The short-range electron-

---

N. Sano  
Institute of Applied Physics, University of Tsukuba,  
1-1-1 Tennoudai, Tsukuba, Ibaraki 305-8573, Japan  
E-mail: sano@esys.tsukuba.ac.jp

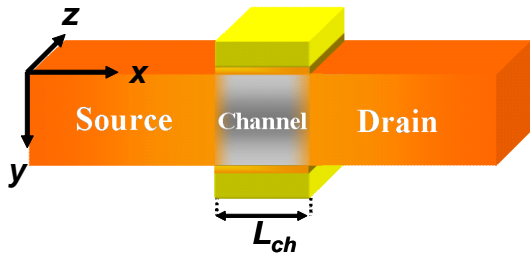


**Fig. 1** Schematic view of the simulated double-gate (DG) MOSFET structure. The donor density of the source and drain regions is  $10^{20} \text{ cm}^{-3}$  and the acceptor density in the channel is  $10^{15} \text{ cm}^{-3}$ . The channel length  $L_{ch}$  varies from 40 nm to 5 nm, whereas the gate insulator (oxide) thickness  $t_{ox}$  and the cross-sectional area of Si channel are fixed at 0.9 nm and  $20 \times 20 \text{ nm}^2$ , respectively. The length of the source or drain region is  $L_{SD} = 40 \text{ nm}$ ,

electron scattering is treated as done in Ref. [9]; it is treated as two-body scattering if the distance between the electrons is shorter than the screening length. The simulation parameters such as deformation potential and coupling constants for phonon scattering are taken from Ref. [8]. The surface roughness scattering is intentionally ignored to clarify the intrinsic effects of the Coulomb interaction on electron transport in ultra-small devices. We also take account of Pauli's exclusion principle for all short-range scattering by employing the rejection technique with the Fermi-Dirac distribution [9]. In fact, this is crucial to properly simulate the degeneracy of electron gas under high electron concentrations. Unless Pauli's exclusion principle is included in MC simulations, electrons would relax *locally* to the Maxwell-Boltzmann distribution due to the fact that electrons are treated as point particles. As a result, the Fermi-Dirac distribution in high-doped source and drain regions could never be achieved in such MC simulations.

The device structure employed for the present MC simulations is the DG-MOSFETs with various channel lengths ( $L_{ch} = 5$  to 40 nm), as schematically depicted in Fig. 1. Relatively large cross-sectional area ( $20 \times 20 \text{ nm}^2$ ) of the device is used to avoid considering the quantum effects associated with confinement. The donor density of the source and drain regions is assumed to be  $10^{20} \text{ cm}^{-3}$  and the acceptor density in the channel is  $10^{15} \text{ cm}^{-3}$ . We would like to stress that the simulation region needs to be large enough that the electron velocity distribution at the source and drain contacts should relax to quasi-equilibrium distributions. In the present study, the length of the source or drain region is  $L_{SD} = 40 \text{ nm}$ . This is also a crucial point: The Boltzmann transport equation intrinsically includes energy dissipation [12] and the energy distribution is ought to

relax to the (local) quasi-equilibrium distribution *which is the only known boundary condition we could impose on the Boltzmann transport equation*. Therefore, to be consistent with the boundary condition at the contacts, it is essential to simulate electron transport not only in the channel region but also in the source and drain regions, as we shall discuss in more detail below.

### 3 Incorporation of the Coulomb Interaction under DG-MOSFET

As we have reported elsewhere [10,11], the parameter optimization is of crucial importance to incorporate the Coulomb interaction accurately into the MC simulations. The strategy we have employed is a similar one used in collisionless plasma simulations [6]: We have performed the MC simulations by artificially turning off all energy-dissipating scattering under thermal equilibrium so that the total energy of the system is strictly conserved. Then, the total energy of the system has been monitored during simulations by changing the simulation parameters. This is a very efficient method for parameter optimization to improve the accuracy and stability of the MC simulations. We would like to stress that energy dissipating scattering always stabilizes MC simulations no matter how the simulation parameters are chosen [13]. After careful optimization of simulation parameters such as time step, mesh size, and the size of simulated electrons, our Monte Carlo simulator is now able to reproduce *simultaneously* both the correct mobility under various impurity concentrations and the collective wave motion at the plasma frequency [10,3].

A typical output from the present self-consistent MC simulations of the DG-MOSFET with  $L_{ch} = 20 \text{ nm}$  is shown in Fig. 2, in which the potential profile in the  $xz$ -plane parallel to the gates is shown. Since the doping density in the source and drain is assumed to be  $10^{20} \text{ cm}^{-3}$ , the potential greatly fluctuates and its magnitude is comparable to the energy of plasmon which is about 200 meV. Fourier-transforming the potential fluctuations in the source and drain regions, we obtain the power spectrum of the potential fluctuations, as shown in Fig. 3. We see that a clear peak around the plasma frequency is observed in the power spectrum even under device operation. This implies that the collective motion as represented by plasma oscillations is well simulated in the present 3D MC simulations. Figure 4 shows the potential profile in the channel direction averaged over many planes parallel to the gates. The potential dynamically fluctuates, but the averaged potential is rather flat in high-doped source and drain regions indicating very small resistance. In fact, the mobility under the electron density of  $10^{20} \text{ cm}^{-3}$  is about 90

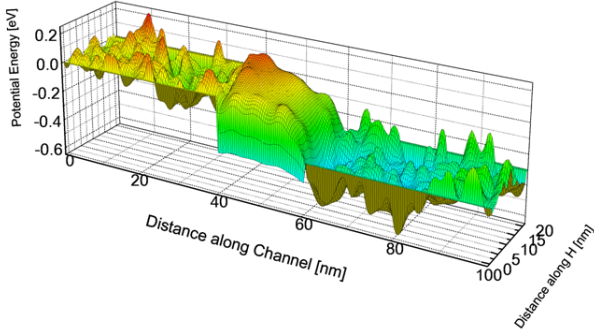


**Fig. 2** Potential profile in the  $xz$ -plane parallel to the gates of DG-MOSFET with  $L_{ch} = 20\text{nm}$ . The magnitude of potential fluctuations in the source and drain is about 200 meV which is comparable to the energy of plasmon for the electron density of  $10^{20}\text{ cm}^{-3}$ .

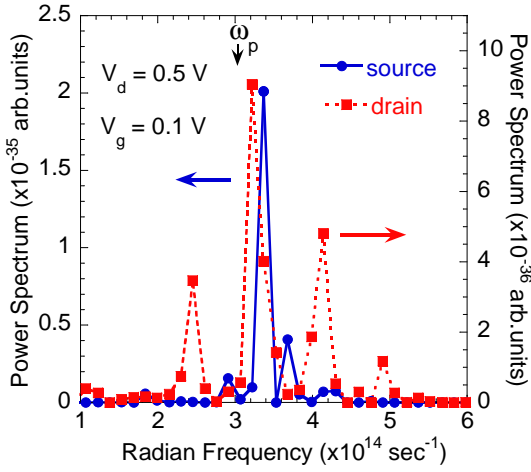


**Fig. 3** Power spectrum of potential fluctuations in the source and drain regions under device operation. A clear peak structure (especially in the source) is observed at the plasma frequency  $\omega_p$  indicated by arrow.

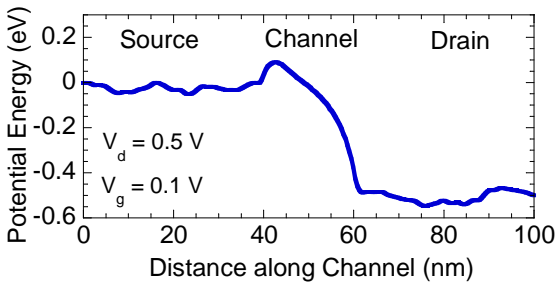


**Fig. 4** Averaged potential profile along the channel direction. The potential drop is very small and nearly flat in the source and drain, consistently with the mobility under high electron concentrations.

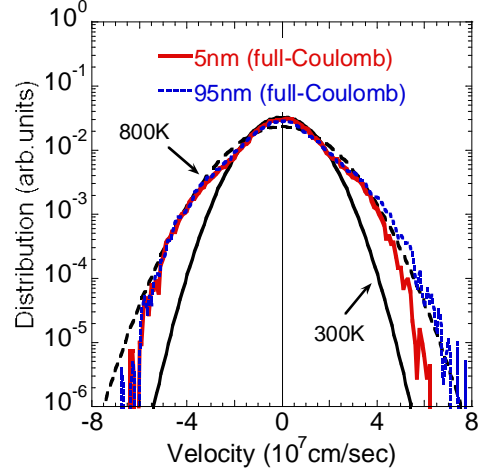


**Fig. 5** Velocity distributions near the source and drain contacts (at  $x = 5$  and  $95\text{ nm}$ ). The solid and empty symbols represent the distributions close to the source and drain contacts, respectively. The Maxwell-Boltzmann distributions with  $T = 300$  and  $800\text{ K}$  are also shown. The distributions near the source and drain contacts coincide with each other, yet the electron temperature is close to  $T = 800\text{ K}$ .

$\text{cm}^2\text{V}^{-1}\text{s}^{-1}$  and, thus, the potential drop in the source and drain regions under the present device structures is expected to be approximately 36 mV. Therefore, we may say that the realistic mobility in high-doped regions is achieved in the present MC simulations, as we have already confirmed in our MC simulations in bulk [10].

Consistency of the boundary condition for the distribution functions is also essential in solving any transport problems. The distribution function we could impose as the boundary condition at the contacts is quasi-equilibrium distribution and its consistency is confirmed in Fig. 5, where time-averaged velocity distributions near the source and drain contacts (at  $x = 5$  and  $95\text{ nm}$ ) are plotted for the DG-MOSFET with  $L_{ch} = 20\text{ nm}$ . The velocity distributions near the source and drain contacts indeed coincide with each other and they are similar to the thermal (Maxwell-Boltzmann) distribution with temperature  $T = 800\text{ K}$ . The reason why the electron temperature is higher than room temperature ( $T = 300\text{ K}$ ) will be discussed in the next section.

## 4 Effects of the Coulomb Interaction on Device Performance

### 4.1 Coulomb Interaction on the Channel Electrons

It has been pointed out that plasmon excitation in high-doped regions by the channel electrons degrades device

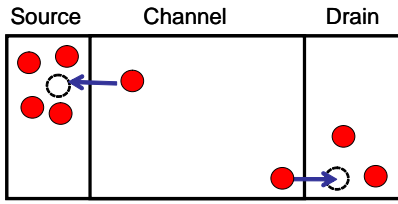


**Fig. 6** Schematic view of the Coulomb correlation between the channel electrons and the electrons in high-doped source or drain regions. The channel electrons close to the source or drain junction are dynamically screened by the Coulomb interaction.

performance in very small MOSFETs [2]. This is interpreted as follows. When the channel electrons reside close to the source or drain region, they repel the electrons in the source or drain region and are attracted by the image charge formed by such dynamical screening, as schematically drawn in Fig. 6. Since dynamical screening is associated with density fluctuations in high-doped regions, it could be simulated only if potential fluctuations are properly taken into account in MC simulations.

In order to study quantitatively the effects of the Coulomb interaction on device performance, the MC simulations under time-averaged potential profile are also carried out, in which the self-consistent loop with the Poisson equation is decoupled. The averaged Coulomb force experienced by an electron inside the device is evaluated by performing the self-consistent MC simulations and the MC simulations under the fixed-potential. The results for the DG-MOSFETs with  $L_{ch} = 20$  and 40 nm are shown in Fig. 7. It is clear that in the case of the self-consistent MC simulations, the channel electrons experience much larger attractive forces near the source and drain junctions than in the cases of the MC simulations under the fixed-potential in both DG-MOSFETs. Notice that the difference in Coulomb force arises no matter what the channel length is. The important difference between the long and short channel devices is, however, that as the channel length shrinks, the Coulomb force due to the image charge begins to alter the entire potential profile in the channel region. This is clearly observed in Fig. 7 where the Coulomb force experienced by the channel electrons under the self-consistent MC simulations is slightly reduced in the channel region, compared with the MC simulations under the fixed-potential.

#### 4.2 Consistency of the Boundary Condition

Consistency of the boundary condition for the electron energy distribution is achieved under the self-consistent

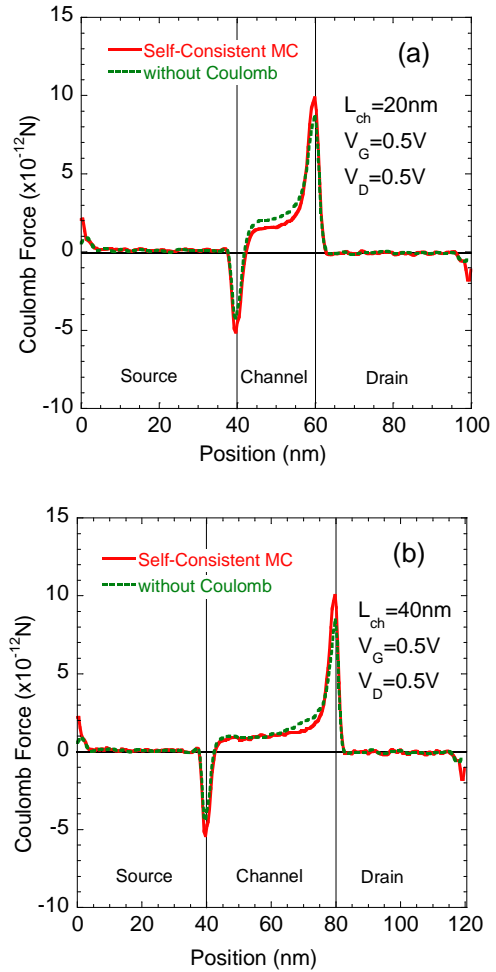


**Fig. 7** Averaged force experienced by an electron due to the long-range part of the Coulomb interaction inside the DG-MOSFETs with (a)  $L_{ch} = 20$  nm and (b)  $L_{ch} = 40$  nm. The self-consistent MC results and the fixed potential MC results are represented by the solid and dotted lines, respectively.

MC simulations, as shown in Fig. 8 where energy distributions close to the source and drain contacts obtained from the MC simulations with and without the full Coulomb interaction are plotted. As we have already pointed out above, the energy distributions near the source and drain contacts ( $x = 5$  and 95 nm) coincide with each other for the self-consistent MC simulations and are close to thermal distribution with  $T = 800$  K. The energy distribution differs from the Fermi-Dirac distribution at room temperature ( $T = 300$  K) because the present energy distribution is plotted with respect to the kinetic energy with the effective density of states which includes the band-tailing effects associated with potential fluctuations. If the effective density of states is de-convoluted from the energy distribution, the energy

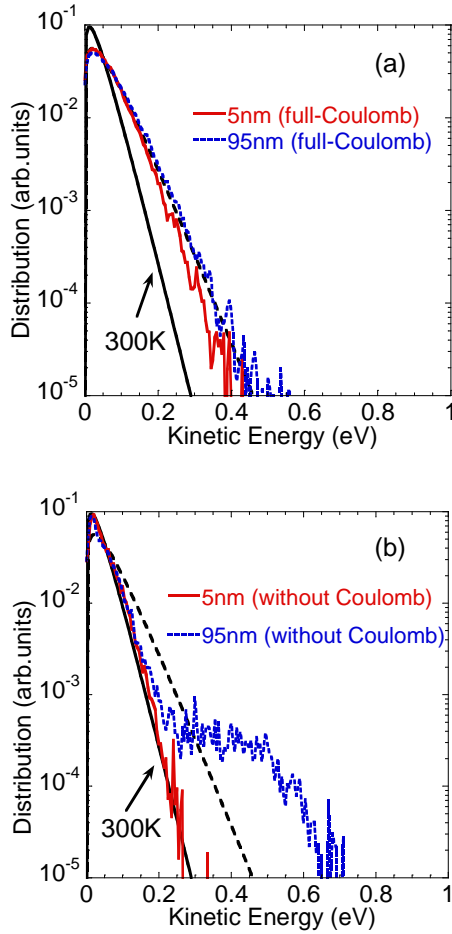


**Fig. 8** Energy distributions close to the source and drain contacts ( $x = 5$  and  $95$  nm) from the MC simulations (a) with the full Coulomb interaction and (b) without the Coulomb interaction. The Maxwell-Boltzmann distributions with  $T = 300$  and  $800$  K are also shown with solid and dotted lines, respectively.

distribution coincides with the Fermi-Dirac distribution with  $T = 300$  K, as already demonstrated in Ref. [1].

We would like to stress that consistency of the boundary condition is achieved only if the Coulomb interaction is properly included in MC simulations. Since the channel electrons are injected into the drain with high kinetic energy comparable to the applied drain voltage, the accurate relaxation processes are essential to obtain realistic transport in the drain region. As seen from Fig. 8 (b) where the MC simulations are carried out under the fixed potential, the momentum and energy relaxations are too weak in the drain to achieve the realistic thermalization processes unless the Coulomb interaction is included. As a result, the energy distribution near the drain contact ( $x = 95$  nm) greatly deviates from the quasi-equilibrium distribution and the boundary condition imposed at the contacts is hard to be satisfied unless the Coulomb interaction (espe-

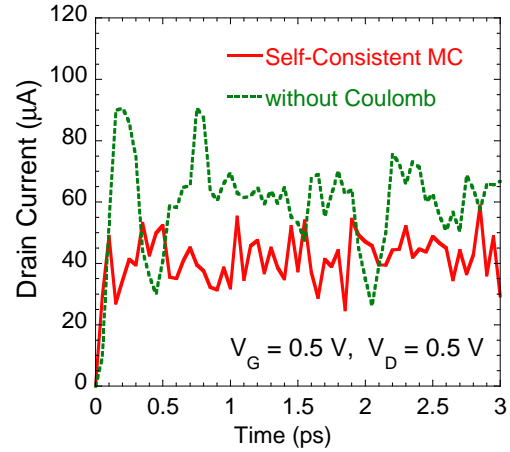


**Fig. 9** Time evolution of the drain current from the self-consistent MC simulation (solid curve) and the fixed potential MC simulation (dotted curve) for the DG-MOSFETs with  $L_{ch} = 20$  nm.

cially, the dynamical potential fluctuations) are taken into account. In addition, we should notice that the energy distribution near the source contact ( $x = 5$  nm) from the fixed potential MC simulations is very close to thermal distribution with  $T = 300$  K in Fig. 8 (b). This implies that the degeneracy of electron gas in the source region cannot be properly simulated without the Coulomb interaction in spite of Pauli's exclusion principle for phonon scattering.

Inconsistency of the boundary conditions near the source and drain contacts induces artificial current flow in the entire device regions because complete-absorption boundary condition is implicitly imposed at the contacts in such MC simulations. This leads to an overestimation of the drain current under the fixed potential MC simulations. Since the channel electrons in longer devices lose their kinetic energy through phonon scattering in the channel region, the details of the energy relaxation processes in the drain region do not matter on device performance, i.e., device performance is entirely determined by the channel mobility. However, electron transport becomes quasi-ballistic in ultra-small devices and, thus, electron transport in the source and drain regions as well as in the channel region greatly affects the current-voltage characteristics. Figure 9 shows the time evolution of the drain current from the self-consistent MC simulations and the fixed potential MC simulations without the Coulomb interaction of the DG-MOSFETs with  $L_{ch} = 20$  nm. The fixed potential MC overestimates the drain current by about 40 %. The reduction of the Coulomb force experienced by the channel electrons and consistency of the boundary condition in the

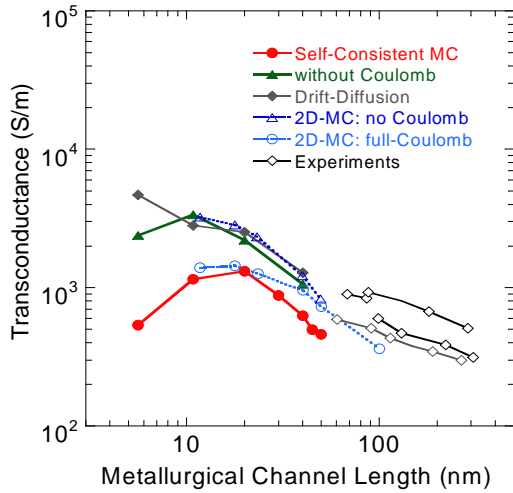


**Fig. 10** Transconductance obtained from the MC simulations with and without the Coulomb interaction (solid marks with solid curves) as a function of the metallurgical channel length. The previous two-dimensional MC simulations with and without the Coulomb interaction (empty marks with dotted curves) are also shown along with some experimental results (empty marks with solid curves).

self-consistent MC simulations would, therefore, reduce the drain current in the DG-MOSFET with  $L_{ch} = 20$  nm, compared with that from the fixed potential MC simulations. In fact, we have confirmed that there is no significant difference in drain current for the DG-MOSFET with  $L_{ch} = 40$  nm between the MC simulations under the self-consistent potential and under the fixed potential [14].

#### 4.3 Device Performance Degradation

The transconductance obtained from the two different MC simulations, with and without the Coulomb interaction, is shown as a function of the metallurgical channel length in Fig. 10. The previous two-dimensional MC simulations with and without the Coulomb interaction [1] are also shown with some experimental results. Our results are very similar to the previous MC results. The device performance is indeed degraded as the channel length is around or below  $L_{ch} = 20$  nm. Since the present MC simulations do not include the surface roughness scattering, performance degradation is entirely intrinsic. The degradation is most significant when the MC simulations are carried out self-consistently. Therefore, the Coulomb interaction indeed degrades device performance as the channel length becomes below 20 nm or so, as first predicted in Ref. [1]. Finally, we would like to stress that the transconductance

is reduced even if the Coulomb interaction is ignored. This is sharp contrary to the prediction made by purely ballistic picture where the reduction of the channel length would improve device performance [15]. Instead, this finding supports the conjecture that scattering is inevitable even in ultra-small channel devices and purely ballistic transport cannot be attained by simply reducing the channel length [16].

## 5 Conclusions

The MC simulations coupled self-consistently with 3D Poisson equation have been carried out under the DG-MOSFET structures. The importance of the Coulomb interaction and the boundary conditions in the MC simulations have been discussed. The Coulomb force experienced by an electron in the device has been directly evaluated by performing the MC simulations with or without the Coulomb interaction, and the plasmon excitation due to the channel electrons has been demonstrated. It has been shown that consistency of the boundary condition is achieved only if the long-range Coulomb interaction is properly taken into account in MC simulations. The transconductance of ultra-small MOSFETs is indeed degraded if the self-consistent potential fluctuations are taken into account and, thus, the Coulomb interaction is a key ingredient for any reliable predictions of device characteristics.

**Acknowledgements** The author is grateful to his previous and present graduate students, T. Uechi, T. Fukui, K. Nakanishi and T. Karasawa, for their contribution. Also, special thanks go to M. V. Fischetti and S. E. Laux for their fruitful discussion and encouragement. This work was partly supported by Grants-in-Aid for Scientific Research on Priority Areas "Post-Scale" (No.18063004) and for Scientific Research (B) (No.2160160) from the Ministry of Education, Culture, Sports, Science, and Technology in Japan.

## References

1. Fischetti, M.V., Laux, S.E.: Long-range Coulomb interactions in small silicon devices. Part I: Performance and reliability. *J. Appl. Phys.* **89**, 1205-1231 (2001).
2. Fischetti, M.V., Jin, S., Tang, T.-w., Asbeck, P., Taur, Y., Laux, S.E., Sano, N.: Scaling MOSFETs to 10 nm: Coulomb effects, source starvation, and virtual source model. *J. Comput. Electron.* **2**, 60-77 (2009).
3. Nakanishi, K., Uechi, T., Sano, N.: Self-Consistent Monte Carlo Device Simulations under Nano-Scale Device Structures: Role of Coulomb interaction, Degeneracy, and Boundary Condition. *IEDM Tech. Dig.* 79-82 (2009).
4. Lugli, P., Ferry, D.K.: Dynamical Screening of Hot Carriers in Semiconductors from a Coupled Molecular-Dynamics and Ensemble Monte Carlo Simulation. *Phys. Rev. Lett.* **56**, 1295-1297 (1986).

- 
5. Kamakura, Y., Ryouke, H., Taniguchi, K.: Ensemble Monte Carlo/Molecular Dynamics Simulation of Inversion Layer Mobility in Si MOSFETs: Effects of Substrate Impurity. *IEICE Trans. Electron.* **E-86-C**, 357-362 (2003).
  6. Hockney, R.W., Eastwood, J.W.: *Computer Simulation using Particles*, p. 267. IOP, Bristol (1988).
  7. Gross, W.J., Vasileska, D., Ferry, D.K.: A novel approach for introducing the electron-electron and electron-impurity interactions in particle-based simulations. *IEEE Electron Device Lett.* **20**, 463-465 (1999).
  8. Jacoboni, C., Lugli, P.: *The Monte Carlo Method for Semiconductor Device Simulation*, p. 218, Springer, Wien (1989).
  9. Fischetti, M.V., Laux, S.E.: Monte Carlo analysis of electron transport in small semiconductor devices including band-structure and space-charge effects. *Phys. Rev. B* **38**, 9721-9745 (1988).
  10. Fukui, T., Uechi, T., Sano, N.: Three-dimensional Monte Carlo Simulation of Electron Transport in Si Including Full Coulomb Interaction. *Appl. Phys. Exp.* **1**, 051407\_1-3 (2008).
  11. Uechi, T., Fukui, T., Sano, N.: 3D Monte Carlo simulation including full Coulomb interaction under high electron concentration regime. *Phys. Status Solidi (c)* **5**, 102-106 (2008).
  12. Resibois, P., de Leener, M.: *Classical Kinetic Theory of Fluids*, p. 73. John Wiley & Sons, New York (1977).
  13. Uechi, T., Fukui, T., Sano, N.: 3D Monte Carlo analysis of potential fluctuations under high electron concentration. *J. Comput. Electron.* **7**, 240-243 (2008).
  14. Sano, N.: Monte Carlo Study of the Coulomb Interaction in Nano-Scale Silicon Devices. *Jpn. J. Appl. Phys.* in press.
  15. Natori, K.: Scaling Limit of the MOS Transistor—A Ballistic MOSFET— *IEICE Trans. Electron.* **E84-C**, 1029-1036 (2001).
  16. Sano, N.: Kinetic of quasiballistic transport in nanoscale semiconductor structures: Is the ballistic limit attainable at room temperature? *Phys. Rev. Lett.* **93**, 246803\_1-4 (2004).